Archive of Applied Mechanics 73 (2004) 650–660 © Springer-Verlag 2004
DOI 10.1007/s00419-003-0315-4

A sufficient criterion for the onset of sprag-slip oscillations

N. Hoffmann, L. Gaul

Summary The objective of the present work is to reexamine the dynamic phenomenon of sprag-slip instability. To that purpose, a model consisting of an elastic beam sliding over a rigid belt at constant speed is set up and investigated. It turns out that there are parameter combinations for which the system does not posess a static solution corresponding to a steady sliding state, neither stable nor unstable, a phenomenon first discovered by Painlevé considering sliding rigid bodies, sometimes referred to as the Painlevé paradox. The nonexistence of a steady sliding state is a sufficient criterion for the appearance of sprag-slip oscillations, since in the corresponding configurations the fundamental behavior of the system is intrinsically dynamic in nature.

Keywords Dynamic system, Friction, Vibration, Self-excitation, Sprag-slip, Instability, Lift-off

1 Introduction

Friction-induced vibrations and friction-related noise belong to common phenomena observable in machine units as different as automotive wheel brakes, squealing railway wheels or even door hinges. In the literature, a number of mechanisms for these phenomena are cited, among those the well-known sliding velocity-dependent friction coefficient, s. e.g. [14], mode coupling, cf. e.g. [1, 2, 8, 9, 16], follower forces and sprag-slip, s. e.g. [5, 10, 18] for reviews. The present work focuses on the last of these mechanisms, first described already in [15]. The fundamental model showing sprag slip-type behavior is the archetypical beam-on-disk setup, where a tilted metal beam is sliding over a rotating metal disk. When the beam's angle of inclination with respect to the disk axis is unfavorable, very vigorous dynamic effects are observable, usually involving intermittent sticking and slipping phases; sometimes the beam may even show a lift-off from the disk.

In the context of the above works on friction-induced vibration, another line of research, although closely related, often remains unmentioned or unnoticed: already in 1872 Jellet, [11], and in 1895 Painlevé, [13], investigated the existence and uniqueness properties of rigid bodies subjected to the Coulomb-type sliding friction, making use of a rigid beam model. It was noticed that, due to the nonlinearity arising from the friction model, both the uniqueness and the existence of solutions for this type of system can be violated, i.e. there is a possibility of multiple solutions and for non-existence of (static) solutions. The phenomenon is called the Painlevé paradox; we refer to [3] for a review discussing the historic aspects of the issue and to [6] for a rather recent treatment using the original Painlevé system as basic model. In the

Received 14 April 2003; accepted for publication 9 November 2003

N. Hoffmann (✉), L. Gaul
Institut A für Mechanik, Universität Stuttgart,
Pfaffenwaldring 9, 70550 Stuttgart
Tel.: 07141/927747
e-mail: norbert.hoffmann2@de.bosch.com

The authors would like to acknowledge multifold support from the acoustics research division FV/FLP of the Robert Bosch GmbH in Gerlingen, Stuttgart. Also the critical and helpful discussions on the topic with Dr. Nils Wagner, Institut A für Mechanik, Universität Stuttgart, are gratefully acknowledged. Special thanks are also due to the Referees of the AAM whose comments helped to add further substantial aspects to the paper.

following, these observations have been mainly taken into account in the development of multibody-system modeling, since multibody systems subjected to friction interaction have to be able to cope with the Painlevé paradox (cf. e.g. [3] for further references), also from the perspective of non-smooth mechanics. Very recently, [12], these phenomena have been considered with respect to a specific aspect of the system dynamics: from the point of view of bifurcation theory, the loss of solution existence corresponds of course to a system transition or bifurcation, demarcating the borderline between distinct regimes of possibly different dynamical behavior. The corresponding system characterization may therefore yield valuable insight into the origins of the phenomena, hard to understand otherwise.

The motivation for the present work lies in the fact that, although sprag slip seems to be a phenomenon known already for a long time now, technical applications are still plagued by sprag slip-type vibrations and noise. The reasons for these enduring problems with sprag slip seem to be twofold. Firstly, although many – and sometimes very intricate – mathematical descriptions and explanations for sprag slip have been given, cf. eg. [15], a simple but general enough, intuitive picture of the basic underlying mechanism allowing e.g. design engineers to derive applicable design measures, seems to be missing still. Secondly, also a simple criterion, allowing a direct and reliable prediction of whether or not a system will show sprag slip, is not at hand yet. The present work therefore reexamines the fundamental dynamical aspects of a system showing sprag slip-type characteristics. It aims at contributing to both an intuitive understanding of sprag slip and to the development of an operational criterion allowing engineers using modern tools like Finite Element Analysis or Elastic Multibody System Simulation to predict whether and when their system will show sprag slip. To that purpose, a model problem is set up, the appearing phenomena are investigated in detail, and a proposal for an approach to deal with sprag slip is derived from the results.

The paper is set up as follows: first, a description for the model system is given in Sec. 2. Then the steady sliding state of the resulting two-degree-of-freedom (2DOF) model is determined in Sec. 3. It turns out that the system does not have a steady sliding state for all parameter combinations. When a steady sliding state is lacking, the system is dynamic by its very nature, and the system's nonlinearities will determine in a very subtle manner the types of limit cycles to be observed. To better understand the reason, why systems of the type considered sometimes lack a steady sliding state, Sec. 4 treats a reduced 1DOF model. From this, an intuitive understanding for the observable dynamics can be gained. The conclusions and an outlook, close the paper.

2
The model problem

It is the objective of the present work to reexamine what is usually called sprag-slip instability in the literature. To do this, we consider the beam-on-belt configuration shown in Fig. 1. The beam of length l is tilted with respect to the vertical by an angle γ and loaded with a constant

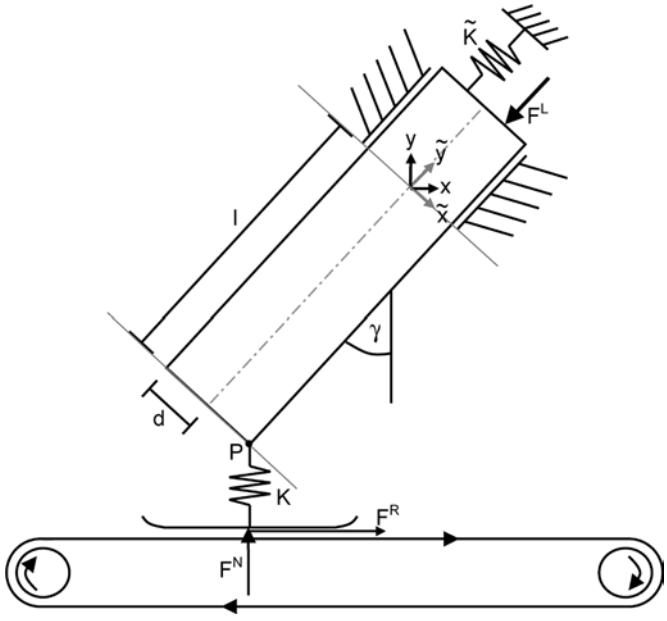

Fig. 1. The model system

force F^L along its neutral axis. At its end it is clamped in the transversal directions and elastically held in the axial direction, modelled by the spring stiffness $\tilde{K}$. The contact to a moving belt system moving with a constant speed v is made via a spring K representing the normal contact stiffness. Coulomb-type friction is assumed, such that $F^R = \mu F^N$. Note also that the point of contact is not located on the neutral axis of the beam, what will also be taken into account. The system will be modelled using two DOF.

For the beam's axial displacement, the equation of motion reads

$$m\ddot{\tilde{y}} + \tilde{K}\tilde{y} = F^L + F^N \cos\gamma + F^R \sin\gamma \ , \tag{1}$$

where the normal and the frictional forces have been projected onto the direction of the undeformed beam's neutral axis. Using the Coulomb friction law and taking into account the relative velocity between the beam tip P and the belt, one obtains

$$m\ddot{\tilde{y}} + \tilde{K}\tilde{y} = F^L + F^N[\cos\gamma + \mu sign(v - \dot{x}_P)\sin\gamma] \ , \tag{2}$$

where $\dot{x}_P$ denotes the tangential velocity component of the beam's contact point. An expression for F^N will be given later.

For the bending of the beam, we will use a modal reduction to the first vibrational bending eigenmode. Although this approximation is rather crude and limits the investigation to a conceptual study, the formal simplification however is convincing and allows for a substantial insight to be gained without getting involved into technical difficulties. Starting from the beam dynamic equation (with beam bending stiffness B and mass density μ_m)

$$Bw'''' + \mu_m \ddot{w} = p(\tilde{y})f(t) \ , \tag{3}$$

the lateral displacement w is expanded into normal modes of the homogeneous system:

$$w = \sum_{j=1}^{\infty} \phi_j(\tilde{y}) q_j \ , \tag{4}$$

where q_j denotes the amplitude if the j-th mode. In our case, the boundary conditions to be applied correspond to the case of a beam clamped at one end at free at the other. This leads to the usual orthogonality conditions for the bending mode shape functions, which can be used to derive the evolution equation for the first mode

$$m_1 \ddot{q}_1 + k_1 q_1 = r_1 \ , \tag{5}$$

where the modal stiffness, mass coefficient and the driving term are given as

$$k_1 = \int_0^l \phi_1'''' \phi_1 B d\tilde{y} = \lambda^4 \int_0^l \phi_1 \phi_1 B d\tilde{y}, \quad m_1 = \int_0^l \phi_1 \phi_1 \mu_m d\tilde{y}, \quad r_1 = \int_0^l \phi_1 p f d\tilde{y} \ . \tag{6}$$

In the following, we will use the equation for the first vibration mode as a representation of the system's bending DOF.

The normal contact force and the frictional force are now modelled as point forces acting on the beam's contact point, such that $p(\tilde{y}) = \delta(\tilde{y} - l)$ can be used to simplify the expression for r_1 to

$$r_1 = \phi_1(l) F^N[-\sin\gamma + \mu sign(v - \dot{x}_P)\cos\gamma] \ . \tag{7}$$

The effects of the moment $F^N \cos\gamma d$ have been neglected here, since presently we will focus on thin beams only. To calculate m_1 and k_1, the analytical solution for $\phi_1(\tilde{y})$ is used

$$\phi_1(\tilde{y}) = C\left[\frac{\cosh\lambda(-\tilde{y}) - \cos\lambda(-\tilde{y})}{\cosh\lambda l + \cos\lambda l} - \frac{\sinh\lambda(-\tilde{y}) - \sin\lambda(-\tilde{y})}{\sinh\lambda l + \sin\lambda l}\right] \ , \tag{8}$$

corresponding to the beam clamped at one end and free at the other, with $\lambda = 1.87510/l$ resulting from the beam equation, cf. eg. [4]. To further simplify the following calculations, we use a scaling corresponding to $\phi_1(l) = 1$. Then q_1 amounts directly to the lateral displacement of the beam's neutral axis at its free end due to the bending deformation. With these assumptions, Eq. (7) for the beam's bending deformation reads

$$m_1\ddot{q}_1 + k_1 q_1 = F^N[-\sin\gamma + \mu sign(v - \dot{x}_P)\cos\gamma] \quad . \tag{9}$$

Here, F^N is still to be determined, which may be done by observing that in the equations of motion derived above F^N depends on the beam's translation $\tilde{y}$ and on its bending state, characterized by q_1. We determine F^N from the compression of the normal contact stiffness K as

$$F^N = -Ky_P\theta(-y_P) \quad , \tag{10}$$

where y_P denotes the displacement of the beam's contact point P normal to the moving belt and θ stands for the step-function, used here to include the possibility of a lift-off. The contribution to y_P from the rigid body displacement $\tilde{y}$ is easily determined as $\tilde{y}\cos\gamma$.

However, for determining the contribution due to the beam bending, some more care has to be taken. For this purpose consider Fig. 2 showing the undeformed and deformed beam configurations. Due to the linear beam theory used, the neutral axis shows only deflections perpendicular to its undeformed configuration. As a consequence of the finite thickness of the beam, however, the contact point P has displacements different from those of the neutral axis even within the linear approximation, since the orientation of the neutral axis in the deformed state differs from that in the undeformed state.

Let's first determine the position $\mathbf{P}'$ of the deformed beam's contact point in the $\tilde{x} - \tilde{y}$ coordinate system aligned with the undeformed beam and located on the neutral axis, as shown in Fig. 2. The new position of the contact point can be determined by rotating the vector $\mathbf{P} = d\hat{\mathbf{e}}_{\tilde{x}}$ by an angle α (which gives the effect of the reorientation of the neutral axis at the beam's end) and then adding the translatory displacement $q_1\hat{\mathbf{e}}_{\tilde{x}}$ due to the bending deformation of the neutral axis:

$$\mathbf{P}' = \mathbf{D}\mathbf{P} + q_1\hat{\mathbf{e}}_{\tilde{x}} \quad . \tag{11}$$

Corresponding to the linear bending which we consider here, the rotation matrix $\mathbf{D}$ is only the linear part of the nonlinear rotation matrix

$$\begin{bmatrix} \cos\alpha & -\sin\alpha \\ \sin\alpha & \cos\alpha \end{bmatrix} = \begin{bmatrix} 1 & -\alpha \\ \alpha & 1 \end{bmatrix} + O(\alpha^2) = \mathbf{D} + O(\alpha^2) \quad , \tag{12}$$

which results in

$$\mathbf{P}' = \begin{bmatrix} 1 & -\alpha \\ \alpha & 1 \end{bmatrix} \begin{pmatrix} d \\ 0 \end{pmatrix} + q_1 \begin{pmatrix} 1 \\ 0 \end{pmatrix} = \begin{pmatrix} d + q_1 \\ \alpha d \end{pmatrix} \quad . \tag{13}$$

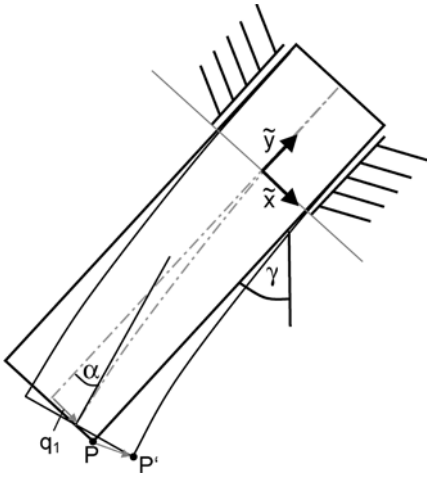

Fig. 2. The bending-induced displacement of the beam's contact point

From this, the relative displacement vector $\mathbf{P}' - \mathbf{P}$ can be calculated as

$$\mathbf{P}' - \mathbf{P} = \begin{pmatrix} q_1 \\ \alpha d \end{pmatrix} . \tag{14}$$

Now it is convenient to express also the angle α as $\alpha = \tilde{\alpha} q_1$ where $\tilde{\alpha} = \phi_1'(l)$. Inserting this in (14) shows that point $\mathbf{P}'$ moves along a straight line, which is however not necessarily parallel to the undeformed beam's bottom edge

$$\mathbf{P}' - \mathbf{P} = q_1 \begin{pmatrix} 1 \\ \tilde{\alpha} d \end{pmatrix} . \tag{15}$$

Already previous beam-on-disk studies, [17], have shown that this (linear !) effect has to be taken into account for adequate modelling of considered systems.

To calculate F^N, a further coordinate transformation of $\mathbf{P}' - \mathbf{P}$ into the $x - y$ coordinate system is needed for which the x-direction is aligned with the belt's plane and the y-direction is orthogonal to it, s. Fig. 1. It is performed using the rotation matrix

$$D^{\tilde{x},\tilde{y}\to x,y} = \begin{bmatrix} \cos\gamma & \sin\gamma \\ -\sin\gamma & \cos\gamma \end{bmatrix} . \tag{16}$$

This yields the coordinates of the contact point in the coordinate system that has to be used to calculate the compression of the contact spring K and the lateral displacement relevant for the stick-slip condition:

$$\mathbf{P}' - \mathbf{P} = \begin{bmatrix} \cos\gamma & \sin\gamma \\ -\sin\gamma & \cos\gamma \end{bmatrix} \begin{pmatrix} 1 \\ \tilde{\alpha} d \end{pmatrix} q_1 = q_1 \begin{bmatrix} \cos\gamma + \tilde{\alpha} d \sin\gamma \\ -\sin\gamma + \tilde{\alpha} d \cos\gamma \end{bmatrix} . \tag{17}$$

To this, the rigid body translation contribution has to be added in order to obtain the position of the contact point as a function of both beam translation and bending

$$\begin{pmatrix} x_P \\ y_P \end{pmatrix} = \begin{pmatrix} \tilde{y}\sin\gamma + q_1(\cos\gamma + \tilde{\alpha} d \sin\gamma) \\ \tilde{y}\cos\gamma + q_1(-\sin\gamma + \tilde{\alpha} d \cos\gamma) \end{pmatrix} . \tag{18}$$

With this result, F^N can be expressed in the variables $\tilde{y}$ and q_1. The resulting system of equations of motion follows

$$\begin{aligned} m\ddot{\tilde{y}} &= -\tilde{K}\tilde{y} + F^L + F^N[\cos\gamma + \mu sign[v - \dot{x}_P]\sin\gamma] \\ &= -\tilde{K}\tilde{y} + F^L + (-K)\theta(-y_P)[\tilde{y}\cos\gamma - q_1(\sin\gamma - \tilde{\alpha} d\cos\gamma)][\cos\gamma + \mu sign(v - \dot{x}_P)\sin\gamma] , \\ m_1\ddot{q}_1 &= -k_1 q_1 + F^N[-\sin\gamma + \mu sign[v - \dot{x}_P]\cos\gamma] \\ &= -k_1 q_1 + (-K)\theta(-y_P)[\tilde{y}\cos\gamma - q_1(\sin\gamma - \tilde{\alpha} d\cos\gamma)][-\sin\gamma + \mu sign(v - \dot{x}_P)\cos\gamma] . \end{aligned} \tag{19}$$

These lengthy expressions may easily be brought into the generic form

$$\begin{pmatrix} m\ddot{\tilde{y}} \\ m_1\ddot{q}_1 \end{pmatrix} + \begin{bmatrix} K_{11} & K_{12} \\ K_{21} & K_{22} \end{bmatrix} \begin{pmatrix} \tilde{y} \\ q_1 \end{pmatrix} = \begin{pmatrix} F^L \\ 0 \end{pmatrix} , \tag{20}$$

where the coefficients of the stiffness matrix can easily be identified. Note however that they depend on the system's state: due to friction and the possibility of a lift-off, the present system is typically piecewise-linear, in which the restoring forces are nonconservative. Due to the presence of friction, we have $K_{12} \neq K_{21}$.

3
The 2DOF problem: the static solution for steady sliding

In the present section we consider the system allowing both bending and translation as described by Eqs. (19) and (20). We determine first the static solution (if possible), i.e. what

usually is called the steady sliding state. For simplicity we restrain parameter variations to the two key parameters: the friction coefficient μ and the beam's inclination angle γ. All other parameters are set to the fixed values $l = 150$ mm, $d = 5$ mm, $m = 2000$ g, $\mu_m = 0.27$ g/mm, $K = 1.0 \times 10^7$ N/mm, $\tilde{K} = 1.0 \times 10^3$ N/mm and $F^L = -10$ N, which correspond qualitatively to values that can be obtained in typical experiments, cf. e.g. [2].

Looking for the steady sliding state, i.e. the static solution of (19), means setting all temporal derivatives to zero and solving the resulting algebraic system. Note first that for this purpose all *sign*-terms can be set to one, since for the static state to be determined also $\dot{x}_P$ will vanish. Then note that two mutually exclusive states of the system have to be considered, depending on whether the beam is in contact with the belt ($y_P < 0$) or not ($y_P > 0$).

For $y_P < 0$, the equations for the static state read:

$$\begin{aligned} &\tilde{y}[-\tilde{K}+(-K)\cos\gamma(\cos\gamma+\mu\sin\gamma)]+q_1[-(\sin\gamma-\tilde{\alpha}d\cos\gamma)(\cos\gamma+\mu\sin\gamma)]=-F^L \\ &\tilde{y}[(-K)\cos\gamma(-\sin\gamma+\mu\cos\gamma)]+q_1[-k_1+(-K)(\sin\gamma-\tilde{\alpha}d\cos\gamma)(-\sin\gamma+\mu\cos\gamma)]=0\,. \end{aligned} \tag{21}$$

For $y_P > 0$, the system reduces to:

$$\begin{aligned} &\tilde{K}\tilde{y} = F^L \\ &k_1 q_1 = 0\ . \end{aligned} \tag{22}$$

However, Eqs. (22) do not have a solution with the constraint $y_P > 0$ (i.e. no contact) for $F^L < 0$ and $0 < \gamma < \pi/2$, what can easily be seen from the definition of y_P in (18). To determine static solutions we will therefore in the following solve the linear algebraic system (21). After a solution is obtained, it must be checked, if the resulting values of $\tilde{y}$ and q_1 do in fact respect the condition $y_P < 0$. Should that not be the case, the system does not have a steady sliding state.

Figure 3 shows the static equilibrium results of $\tilde{y}$, q_1 and y_P vs. the beam's angle of inclination γ for $\mu = 0.0$, 0.2, 0.4, 0.6 and 0.8. First note that the result for $\mu = 0.0$ is nothing but the well-known beam bending result viewed in a somewhat tilted coordinate system: for all angles γ the beam is tilted as if its tip were trying to align itself with the contact surface. For $\mu = 0.2$, however, there is a parameter regime of small γ, where the beam tip is rather trying to get into an upright position with respect to the belt, due to the friction force exerting bending. For larger γ, however, the bending known from $\mu = 0$ is recovered. Note also that there is a small range of parameters at small γ where $\tilde{y}$ is positive, i.e. the beam as a rigid body backs somewhat off from the belt, and only the instantaneous beam bending still allows the beam to stay in contact with the belt. For $\mu = 0.4$, this effect becomes even more apparent: there is a rather wide range of the inclination angle for which $\tilde{y}$ is positive, i.e. with respect to the longitudinal displacement the beam is somewhat lifted from the surface; the contact is nevertheless sustained, since the bending deflection is so strong that the contact point on the beam's tip stays attached to the moving belt.

The fundamental surprise of this simple analysis, however, appears for friction coefficients $\mu > 0.45$, e.g. for $\mu = 0.6$. Now a range of the inclination angle appears, for which our analysis indicates $y_P > 0$, which means that the beam's tip point is not attached to the belt any more. We have noted already that the analysis performed does not lead then to a valid static solution, and we have to conclude that for this range of γ there is no static solution, no steady sliding state at all. Looking at the results for $\mu = 0.8$ it turns out that the parameter regime for which no static solution exists further increases with increasing μ. To clarify the situation Fig. 4 shows the parameter regime for which no static solution, no steady sliding state exists. Apparently something is happening for $\mu > 0.45$, with the consequence that for certain inclination angles of the beam the whole system lacks the property of having a static solution.

To understand the situation better, Fig. 5 shows results of an eigenvalue analysis of the system and some force-vector plots, since a direct graphical representation of the four-dimensional phase-space is of course not possible. For the eigenvalue analysis, the homogeneous part of Eqs. (19) is solved under the restraints $y_P < 0$, i.e. in the case of closed contact, and for $\dot{x}_P < v$, i.e. at small vibration amplitude, using the exponential ansatz

$$\begin{pmatrix} \tilde{y} \\ q_1 \end{pmatrix} = \begin{pmatrix} \tilde{y}^0 \\ q_1^0 \end{pmatrix} \exp(i\omega t)\ . \tag{23}$$

The left column of Fig. 5 shows the resulting lowest eigenvalue ω^2, corresponding to the beam bending mode, for $\mu = 0.0$, 0.4 and 0.8 vs. the beam inclination angle γ. Note that the friction-

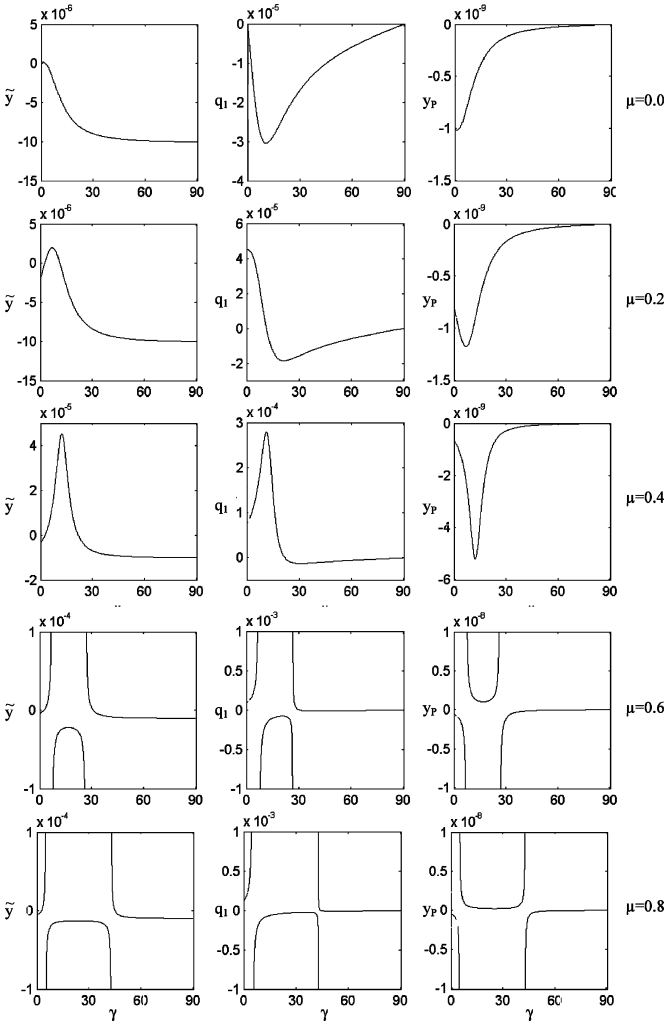

Fig. 3. Static equilibrium results for $\tilde{y}$, q_1 and y_P vs. the beam's angle of inclination γ at $\mu = 0.0$, 0.2, 0.4, 0.6 and 0.8 (from top to bottom)

related stiffness effects lead to a decrease of the natural frequency of beam bending for small inclinations; for $\mu = 0.8$ there even is a range of angles for which the beam bending mode has become monotonically unstable ($\omega^2 < 0$). This instability always coincides with the lack of a steady sliding state, as can be shown by simple algebra.

We will not focus, however, on spectral characteristics here, but try to point out what does this change in the stability characteristics in conjunction with the loss of a steady sliding state mean for the dynamics of the system. Since the phase state of the system is four dimensional, the corresponding flow geometry can not be simply plotted in two-dimensional graphs. Instead, we have chosen to represent the force-vector fields arising from Eqs. (21) and (22) for a fixed inclination angle of $\gamma = 15^\circ$. In a first step, we consider Eqs. (21), disregarding that it is valid for $y_P < 0$ only. The force-vector fields for $\mu = 0.0$, 0.4 and 0.8 are shown in the middle column of Fig. 5. The force-vector fields of the complete system (corresponding to either Eqs. (21) or (22), depending on whether $y_P < 0$ or $y_P > 0$) are represented in the right column of Fig. 5.

Now, how can the phenomenon of the disappearance of the static solution be understood? In Sec. 4, we will give a rather intuitive explanation, using a simplified 1DOF model. Here,

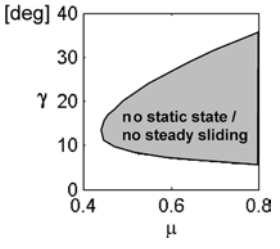

Fig. 4. Parameter regime in γ vs. μ, for which no static solution, i.e. no steady sliding state exists

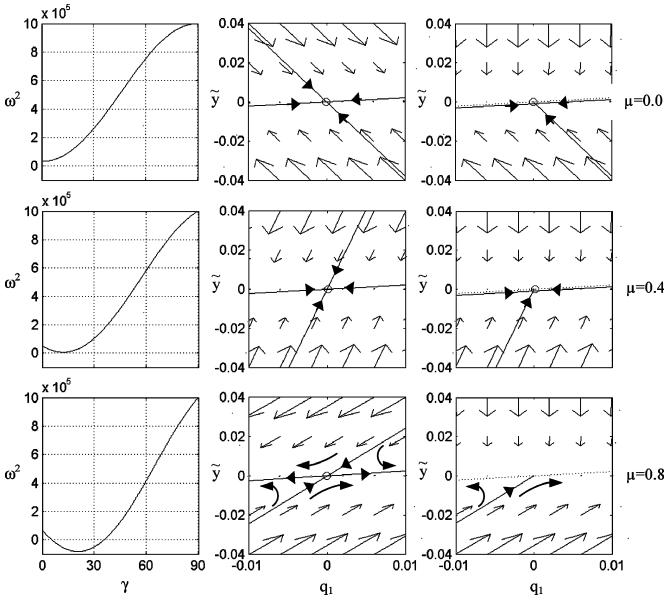

Fig. 5. Results for friction coefficients $\mu = 0.0$, 0.4 and 0.8 (from top to bottom) Left column: Eigenvalues ω^2 for the beam's first bending mode vs. the inclination angle γ. Middle column: Force-vector fields corresponding to Eq. (21). Also shown are the separatrices corresponding to the eigenvectors (straight lines with arrows indicating temporal evolution) and the static solutions (small circle). Right column: Force-vector fields of the complete system (21 + 22). The dotted line represents the borderline to a lift-off. The vectors in the lift-off-position are magnified for better visibility

however, we choose a mathematical perspective and give an answer in terms of the dynamical systems theory. Basically, the phenomenon described can be understood as a peculiar interplay of two aspects: First, there is the possibility of a lift-off in the system. Second, there are the peculiarities with the system's fixed points, i.e. its static solutions. We have seen that there is a range of inclination angles for which no static solution exists, due to the fact that the contact spring K can not be brought into a stretched state. Instead, the beam takes off and the system's discontinuity forces the examiner to switch the equations of motion. Let us now for a while assume that the lift-off does not take place and that the statics of the system is therefore fully described by Eqs. (21) that apply otherwise only for $y_P < 0$. Of course, there is always a static solution then, marked through a circle in the middle column of Fig. 5. But what about the stability properties of these solutions, the stability of the fixed points? Figure 5 (left column) gives the stability results for $\mu = 0.0$, 0.4 and 0.8. It turns out that the static solutions corresponding to $y_P > 0$, which appear for the higher values of μ only, are unstable since one of the two eigenmodes of the system has turned unstable. Mathematically, an increase in μ transforms the stable static solution into one that is unstable with respect to one monotonically unstable mode. In terms of dynamical systems notation, a stable 'elliptic' fixed point has been transformed into an unstable 'hyperbolic' one, s. e.g. [7] for further details.

The behavior described up to now is not something very peculiar from the perspective of the system dynamics. What makes the system considered interesting, however, is its discontinuous response due to the lift-off. It comes into play rather intricately: when the lift-off condition is taken into account again, it erases all hyperbolically unstable fixed points from the full system, since they would correspond to a stretched contact spring, which is physically inadmissible. In the phase space nevertheless the hyperbolic fixed point's signature still remains, s. the lowest graph in the right column of Fig. 5. In the four-dimensional phase space the lift-off condition $y_P = 0$ forms a hypersurface cutting the space into two parts. The part with $y_P < 0$ (representing all situations when the beam is in contact with the belt) looks as if there were a hyperbolically unstable fixed point around somewhere; however, it is not there any more, since for $y_P > 0$ another type of phase space, which contains no fixed point at all, has been stitched to the hypersurface $y_P = 0$.

To summarize this analysis we state that for certain parameter combinations the system considered does not have a static solution, corresponding to a steady sliding state, which can be traced back to the combination of the system's stability characteristics and its dynamic discontinuity related to the possibility of a lift-off.

On the first sight, this behavior may be merely of academic interest. However, having understood this leads to a number of immediate consequences, the most significant of which is that systems without a steady sliding state always show limit-cycle behavior, irrespective of how strong the applied damping is.

Before we discuss this and other consequences, we will consider a simplified 1DOF problem, which should elucidate from an intuitive perspective the underlying mechanism.

4
The 1DOF problem

The 2DOF problem presented in Sec. 3 has been described as it naturally emerges from modelling of the beam-on-disk setup. It has been shown that for certain parameter combinations the system does not have a static, steady sliding state, not even an unstable one, such that the system is per se dynamic in nature.

The mathematical explanation for this phenomenon given above will be given now a more intuitive treatment in terms of force and stiffness characteristics. For this purpose, we put a constraint on the system in the longitudinal axis, assuming $\tilde{y} = const.$ Then additional bearing forces will appear along the beam's longitudinal axis that restrain the beam in its position. For the dynamical behavior, instead of Eqs. (19), a single equation in q_1 remains to be valid

$$m_1\ddot{q}_1 + q_1[k_1 - \theta(-y_P)K(\sin\gamma - \tilde{\alpha}d\cos\gamma)(-\sin\gamma + \mu\cos\gamma)] = -\theta(-y_P)\tilde{y}K\cos\gamma[-\sin\gamma + \mu\cos\gamma] \quad . \tag{24}$$

When the beam is clamped in a position allowing no contact with the belt, $q_1 = 0$ is the trivial static solution. If the clamping is such that contact is enforced ($y_P < 0$), the static solution can be obtained from

$$q_1[k_1 - K(\sin\gamma - \tilde{\alpha}d\cos\gamma)(-\sin\gamma + \mu\cos\gamma)] = -\tilde{y}K\cos\gamma(-\sin\gamma + \mu\cos\gamma) \quad , \tag{25}$$

given that the condition $y_P < 0$, i.e.

$$\tilde{y}\cos\gamma - q_1(\sin\gamma - \tilde{\alpha}d\cos\gamma) < 0 \quad , \tag{26}$$

is fulfilled. Figure 6 shows exemplary solutions to Eq. (25) as a function of the tilting angle γ, assuming $\mu = 0.6$, $\tilde{y} = -0.1$ mm, $K = 1000$ N/mm and otherwise the same constants as in Sec. 3. It turns out that a picture largely analogous to the 2DOF case, Fig. 3, emerges: again there is an angle interval for which the solution of (25) does not satisfy the contraint (26), i.e. there is no static, steady sliding state within this interval.

In close analogy to the 2DOF case, the static solution of (25) is unstable in exactly the same parameter regime in which it does not satisfy (26), cf. Fig. 6. The 1DOF model, however, allows us to give a simple intuitive explanation for this, at the first sight rather peculiar, system behavior. To that purpose, reconsider Eq. (25). The left-hand side consists of the product of the displacement q_1 with the corresponding stiffness coefficient containing a contribution of the friction force. The key feature of this friction-related term is that it may give a diminishing contribution to the total stiffness coefficient, that may even render the total stiffness coefficient negative, i.e. the system may become unstable.

The right-hand side term, due to the constraint on the system, represents a given load on the system. The beam reacts to this load by building up a deflection q_1 which is correlated to a structural restoring force. With the deflection there goes along an increase in the normal force: by bending the beam in the positive direction, its contact tip – due to the axial constraint on the beam – is pushed further into the contact spring. Therefore the normal force, and by that also the friction force, do increase and interfere with the purely structural restoring forces. When the friction coefficient is large enough to allow for a strong enough friction force this effect may lead to self-excitation: the beam bends to set up a restoring force, but instead of reaching a static equilibrium position also the accelerating friction force increases and may even overcompensate the increasing structural restoring force. The system is then continuously accelerated and the increasing bending follows unlimited, at least in the linear model.

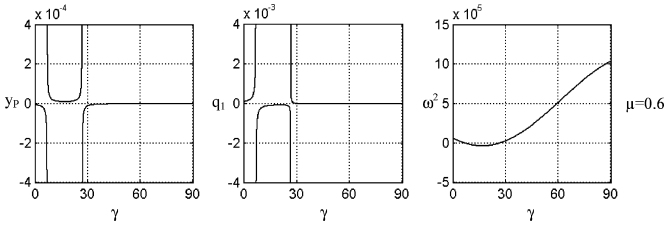

Fig. 6. Values of y_P (left), q_1 (middle) and ω^2 (right) vs. the inclination angle γ for the 1DOF model as obtained from Eq. (25)

Having grasped this fundamental feature of the system's dynamic behavior, a comparison with Painlevé's and Spurr's criteria is appropriate. According to these earlier investigations, [13], [15], the instability condition for rigid rods subjected to Coulomb friction amounts to $\mu > \tan\gamma$. It is argued that for $\mu = \tan\gamma$ large, even infinite forces appear, an effect called 'spragging' by Spurr, and the system is driven into instability. Now, how does this picture fit with the results of the present work? A close look at Eq. (25) gives the answer. For not too small γ (a case we will describe below) the condition $\mu = \tan\gamma$ describes exactly the parameter combination for which the sign of the friction-induced restoring forces of the beam bending, i.e. the term involving the contact stiffness K on the left-hand side of Eq. (25), changes sign, such that for $\mu > \tan\gamma$ it counteracts the structural restoring forces according to k_1. When the system parameters μ or γ cross this border, the whole restoring coefficient of the equation's left-hand side very rapidly goes to zero as an effect of the size of K, leading to unlimited beam bending, as may be observed also from Fig. 6.

Note, however, that the classic reasoning allows an explanation only for the disappearance of a static solution when γ is reduced below a critical value. Using the present elastic beam model, there still remains a parameter interval of very small angles above zero, where there exists a static solution, in contradiction to Spurr's condition. The present approach however allows a simple explanation for this phenomenon as well. For very small γ the beam thickness plays a role, resulting from the factor $\sin\gamma - \tilde{\alpha} d \cos\gamma$ on the left-hand side of Eq. (25). Since both d and $\tilde{\alpha}$ are typically rather small quantities, for reasonably large values of γ both the sign and the value of the term are dominated by the $\sin\gamma$ component. When γ approaches zero however, inevitably a sign change occurs, which renders the system stable again. Thus, the reasoning followed in the present work corresponds well with the condition for instability proposed by Spurr, although, the inclusion of elasticity and the finite beam thickness yield additional effects.

Another, more formal comment seems necessary: systems with negative stiffness coefficients are well known in structural dynamics, cf e.g. the inverted pendulum. Usually, for such systems there still exists a static solution, although it is unstable, as e.g. in the case of the inverted pendulum. In the present case, however, the static state itself (the system's fixed point in mathematical terms) does not exist any more for certain parameter combinations, although its phase space environment still characterizes the system's dynamics. This is the very peculiarity of what is usually called sprag-slip dynamics.

5
Conclusions and outlook

We have seen that in systems like the one considered it is possible that for certain parameter combinations a static solution, i.e. a steady sliding state, does not exist. From this several conclusions have to be drawn for the analysis and treatment of this type of system, especially in technical applications.

First, it has always to be checked whether a static state, a steady sliding state exists under the operational conditions the system is subjected to. In the case of a lacking static solution, the system will inevitably show limit-cycle behavior, which may well be called a sprag-slip oscillation. In this sense, a sufficient condition for detecting sprag-slip oscillations has been revealed. It should be noted that in this case very special care and attention will have to be paid to the system's nonlinearities, since they will crucially influence even the general nature of the resulting vibration. Also, only if a steady sliding state exists, the usual analysis techniques based on linear (or linearized) modelling, like stability analysis of the complex eigenvalue type, are applicable.

Second, measures for quietening a sprag slip-type system will have to be markedly different from systems with a static state: for example, when there is no static solution, simply adding damping will not result in significant improvement of the systems vibration properties, since there just is no quiet static state to which the more damped system might tend to. Quietening a sprag-slip system might therefore mean finding an acceptable dynamical behavior rather than eliminating dynamical behavior in general.

Third, even though it will be very helpful with respect to quietening sprag slip-type systems to eliminate system configurations that inevitably lead to dynamical behavior – as can be characterized by the sufficient condition for dynamical behavior proposed in the present work, it remains a major challenge to work towards necessary criteria. Already from simple 1DOF stick-slip systems it is well known that, as an effect of the peculiarities of the system nonlinearities involved, very intricate and – from an engineering point of view – vicious phenomena like e.g. discontinuous subcritical bifurcations are possible. Necessary criteria for whatever

dynamical state of systems faced with sprag-slip characteristics will therefore demand further efforts, especially with respect to the nonlinear dynamics of the systems under consideration.

These – certainly incomplete – conclusions already show that there is still much work to be done on sprag slip-type systems. Three aspects, however, seem to be of major importance for gaining further understanding: First, the time evolution of sprag-slip oscillations has to be investigated in detail. Especially when situations allowing lift-off are admitted, it will have to be answered, if structural damping will lead to bounded limit cycles, or if even then unbounded solutions do exist. We have not conducted such an analysis for the present model, since we think that, second, the conceptual results of the present study should be reexamined using modelling tools allowing closer representation of realistic technical applications, like e.g. an automotive brake. From this more realistic and technically oriented work certainly much could be learned about actual realizations of sprag slip. Third, the present work sets the motivation for having a close look at relevant system nonlinearities. Although in usual modelling practice nonlinearities are often considered as second-order model components, we have seen that in sprag-slip configurations the system nonlinearities are of primary importance for the system's dynamics, and have to be taken into account even at the simplest level of modelling. The role of nonlinear structural forces (e.g. due to geometric or material effects) as well as of realistic nonlinear contact and friction forces will have to be examined in close detail and will add substantial further facets to the understanding of the sprag-slip phenomenon.

References

1. **Allgaier, R.; Gaul, L.; Keiper, W.; Willner, K.:** Mode lock-in and friction modelling. In: Gaul, L. and Brebbia, C.A. (eds.) Computational methods in contact mechanics IV. WIT Press, Southampton, (1999) 35–47
2. **Allgaier, R.; Gaul, L.; Keiper, W.; Hoffmann, N.:** A study on brake squeal using a beam-on-disc model. Proc Int Modal Analysis Conf - IMAC XXI, Los Angeles, (2002)
3. **Feeny, B.; Guran, A.; Hinrichs, N.; Popp, K.:** A historical review on dry friction and stick-slip phenomena. Appl Mech Rev 51 (1998) 321–341
4. **Gasch, R.; Knothe, K.:** Strukturdynamik. Springer, Berlin-Heidelberg, (1989)
5. **Gaul, L.; Nitsche, R.:** Role of friction in mechanical joints. Appl Mech Rev 54 (2001) 93–105
6. **Génot, F.; Brogliato, B.:** New results on Painlevé paradoxes. Eur J Mech A/Solids 18 (1999) 653–677
7. **Guckenheimer, J; Holmes, P.:** Nonlinear oscillations, dynamical systems, and bifurcations of vector fields. Springer, Berlin, Heildelberg, (1983)
8. **Hoffmann, N.; Fischer, M.; Allgaier, R.; Gaul, L.:** A minimal model for studying properties of the mode-coupling type instability in friction induced oscillations. Mech Res Commun 29 (2002) 197–205
9. **Hoffmann, N; Gaul, L.:** Effects of damping on mode-coupling instability in friction induced oscillations: imperfect merging of modes and viscous instability. Z Angew Math Mech 83 (2003) 524–534
10. **Ibrahim, R.A.:** Friction-induced vibration, chatter, squeal and chaos II: dynamics and modeling. ASME Appl Mech Rev 47 (1994) 227–253
11. **Jellet, J.H.:** Treatise on the theory of friction. Hodges, Foster and Co, (1872)
12. **Leine, R.I.; Brogliato, B.; Nijmeijer, H.:** Periodic motion and bifurcations induced by the Painlevé paradox. Eur J Mech A/Solids 21 (2002) 869–896
13. **Painlevé, M.:** Sur les Lois du Frottement de Glissement, Comptes Rendus de l'Academie des Science 121 (1895) 112–115
14. **Popp, K.; Stelter, P.:** Stick-slip and chaos. Philosophical Trans R Soc London A 332 (1990) 89–105
15. **Spurr, R.T.:** A theory of brake squeal. Proc Automotive Division, Inst Mech Engineers (AD) 1 (1961) 33–40
16. **Tuchinda, A.; Hoffmann, N.P.; Ewins, D.J.; Keiper, W.:** Mode Lock-in Characteristics and Instability Study of the Pin-On-Disc System, Proc Int Modal Analysis Conf - IMAC XX, Kissimee, (2001)
17. **Tuchinda, T.; Hoffmann, N.P.; Ewins, D.J.:** Effect of pin finite width on instability of pin-on-disc systems. Proc Int Modal Analysis Conf - IMAC XXI, Los Angeles, (2002)
18. **Wallaschek, J.; Hach, K.-H.; Stolz, U.; Mody, P.:** A survey of the present state of friction modelling in the analytical and numerical investigation of brake noise generation. Proc ASME Vibration Conf, Las Vegas, (1999) 12–15